

## A High Statistics Search for $\nu_\mu(\bar{\nu}_\mu) \rightarrow \nu_e(\bar{\nu}_e)$ Oscillations in the Small Mixing Angle Regime

A. Romosan,<sup>2</sup> C. G. Arroyo,<sup>2</sup> L. de Barbaro,<sup>5</sup> P. de Barbaro,<sup>7</sup> A. O. Bazarko,<sup>2</sup> R. H. Bernstein,<sup>3</sup> A. Bodek,<sup>7</sup> T. Bolton,<sup>4</sup> H. Budd,<sup>7</sup> J. Conrad,<sup>2</sup> R. B. Drucker,<sup>6</sup> D. A. Harris,<sup>7</sup> R. A. Johnson,<sup>1</sup> J. H. Kim,<sup>2</sup> B. J. King,<sup>2</sup> T. Kinnel,<sup>8</sup> M. J. Lamm,<sup>3</sup> W. C. Lefmann,<sup>2</sup> W. Marsh,<sup>3</sup> K. S. McFarland,<sup>3</sup> C. McNulty,<sup>2</sup> S. R. Mishra,<sup>2</sup> D. Naples,<sup>4</sup> P. Z. Quintas,<sup>2</sup> W. K. Sakumoto,<sup>7</sup> H. Schellman,<sup>5</sup> F. J. Sciulli,<sup>2</sup> W. G. Seligman,<sup>2</sup> M. H. Shaevitz,<sup>2</sup> W. H. Smith,<sup>8</sup> P. Spentzouris,<sup>2</sup> E. G. Stern,<sup>2</sup> M. Vakili,<sup>1</sup> U. K. Yang,<sup>7</sup> and J. Yu<sup>3</sup>

<sup>1</sup> *University of Cincinnati, Cincinnati, OH 45221*

<sup>2</sup> *Columbia University, New York, NY 10027*

<sup>3</sup> *Fermi National Accelerator Laboratory, Batavia, IL 60510*

<sup>4</sup> *Kansas State University, Manhattan, KS 66506*

<sup>5</sup> *Northwestern University, Evanston, IL 60208*

<sup>6</sup> *University of Oregon, Eugene, OR 97403*

<sup>7</sup> *University of Rochester, Rochester, NY 14627*

<sup>8</sup> *University of Wisconsin, Madison, WI 53706*

(May 20, 2018)

Limits on  $\nu_\mu(\bar{\nu}_\mu) \rightarrow \nu_e(\bar{\nu}_e)$  oscillations based on a statistical separation of  $\nu_e N$  charged current interactions in the CCFR detector at Fermilab are presented.  $\nu_e$  interactions are identified by the difference in the longitudinal shower energy deposition pattern of  $\nu_e N \rightarrow eX$  versus  $\nu_\mu N \rightarrow \nu_\mu X$  interactions. Neutrino energies range from 30 to 600 GeV with a mean of 140 GeV, and  $\nu_\mu$  flight lengths vary from 0.9 km to 1.4 km. The lowest 90% confidence upper limit in  $\sin^2 2\alpha$  of  $1.1 \times 10^{-3}$  is obtained at  $\Delta m^2 \sim 300 \text{ eV}^2$ . For  $\sin^2 2\alpha = 1$ ,  $\Delta m^2 > 1.6 \text{ eV}^2$  is excluded, and for  $\Delta m^2 \gg 1000 \text{ eV}^2$ ,  $\sin^2 2\alpha > 1.8 \times 10^{-3}$  is excluded. This result is the most stringent limit to date for  $\Delta m^2 > 25 \text{ eV}^2$  and it excludes the high  $\Delta m^2$  oscillation region favoured by the LSND experiment. The  $\nu_\mu$ -to- $\nu_e$  cross-section ratio was measured as a test of  $\nu_\mu(\bar{\nu}_\mu) \leftrightarrow \nu_e(\bar{\nu}_e)$  universality to be  $1.026 \pm 0.055$ .

PACS numbers: 14.60.Pq, 13.15.+g

The existence of neutrino mass and mixing would have important implications for fundamental problems in both particle physics and cosmology. These include violation of lepton family number conservation, the mass of the universe, and the observed neutrino deficits from the sun and from atmospheric sources. Neutrino oscillations are a necessary consequence of non-zero neutrino mass and mixing since neutrinos are produced and detected in the form of weak-interaction eigenstates whereas their motion as they propagate from the point of production to their detection is dictated by the mass eigenstates [1]. In the two-generation formalism, the mixing probability is:

$$P(\nu_1 \rightarrow \nu_2) = \sin^2 2\alpha \sin^2 \left( \frac{1.27 \Delta m^2 L}{E_\nu} \right) \quad (1)$$

where  $\Delta m^2$  is the mass squared difference of the mass eigenstates in  $\text{eV}^2$ ,  $\alpha$  is the mixing angle,  $E_\nu$  is the incoming neutrino energy in GeV, and  $L$  is the distance between the point of creation and detection in km.

To date the best limits from accelerator experiments for  $\nu_\mu \rightarrow \nu_e$  oscillations come from fine-grained calorimetric (e.g.: BNL-E734 [2], BNL-E776 [3]) or fully active detectors (e.g. KARMEN [4], LSND [5]) searching for quasi-elastic charged current production of electrons. The LSND experiment, using a liquid scintillator neutrino target, has reported a signal consistent with  $\bar{\nu}_\mu \rightarrow \bar{\nu}_e$  oscillations at a  $\sin^2 2\alpha \approx 10^{-2}$  and  $\Delta m^2 \gtrsim 1 \text{ eV}^2$  [5]. The CCFR collaboration has previously reported a limit on  $\nu_\mu \rightarrow \nu_e$  oscillations using the ratio of neutral to charged current neutrino events comparable in sensitivity to the above mentioned limits [6].

In this report we present new limits on  $\nu_\mu \rightarrow \nu_e$  oscillations based on the statistical separation of  $\nu_e N$  charged current interactions.

The CCFR detector [7,8] consists of an 18 m long, 690 ton total absorption target calorimeter with a mean density of  $4.2 \text{ g/cm}^3$ , followed by a 10 m long iron toroidal spectrometer. The target consists of 168 steel plates, each  $3 \text{ m} \times 3 \text{ m} \times 5.15 \text{ cm}$ , instrumented with liquid scintillation counters placed every two steel plates and drift chambers spaced every four plates. The separation between scintillation counters corresponds to 6 radiation lengths, and the ratio of electromagnetic to hadronic response of the calorimeter is 1.05. The toroid spectrometer is not directly used in this analysis which is based on the shower profiles in the target-calorimeter.

The Fermilab Tevatron Quadrupole Triplet neutrino beam is a high-intensity, non-sign-selected wideband beam with a  $\nu : \bar{\nu}$  flux ratio of about 2.5 : 1 and usable neutrino energies up to 600 GeV. The production target is located 1.4 km upstream of the neutrino detector and is followed by a 0.5 km decay region. The resulting neutrino energy spectra for  $\nu_\mu$ ,  $\bar{\nu}_\mu$ ,  $\nu_e$ , and  $\bar{\nu}_e$  induced events are shown in Figure 1. The beam contains a 2.3% fraction of electron neutrinos, 82% of which are produced

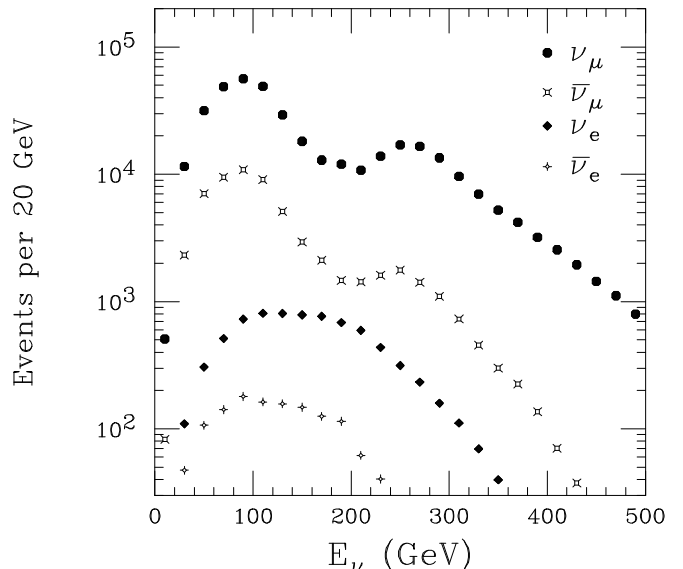


FIG. 1. Neutrino energy spectra for  $\nu_\mu$ ,  $\bar{\nu}_\mu$ ,  $\nu_e$ , and  $\bar{\nu}_e$  at the CCFR detector for the FNAL wideband neutrino beam (Monte Carlo based on relative  $\nu_\mu$  and  $\bar{\nu}_\mu$  fluxes).

from  $K^\pm \rightarrow \pi^0 e^\pm \bar{\nu}_e^{(-)}$ .

The neutrino interactions observed in the detector can be divided into three classes depending on the type of the incoming neutrino and on the interaction type:

1.  $\nu_\mu N \rightarrow \mu^- X$  ( $\nu_\mu$  charged current (CC) events).
2.  $\nu_{\mu,e} N \rightarrow \nu_{\mu,e} X$  ( $\nu_{\mu,e}$  neutral current (NC) events).
3.  $\nu_e N \rightarrow e X$  ( $\nu_e$  CC events).

All three types of neutrino interactions initiate a cascade of hadrons that is registered by the drift chambers and scintillation counters. The  $\nu_\mu$  CC events are characterized by the presence of a muon produced in the final state which penetrates beyond the end of the hadron shower, depositing energy characteristic of a minimum ionizing particle [7] in a large number of consecutive scintillation counters. Conversely, the electron produced in a  $\nu_e$  CC event deposits energy in a few counters immediately downstream of the interaction vertex which changes the energy deposition profile of the shower. The electromagnetic shower is typically much shorter than the hadron shower and the two cannot be separated for a  $\nu_e$  CC event.

In this analysis four experimental quantities are calculated for each event: the length, the transverse vertex position, the visible energy and the shower energy deposition profile. The event length is determined to be the number of scintillation counters spanned from the event vertex to the last counter with a minimum-ionizing pulse height. The mean position of the hits in the drift chamber immediately downstream of the interaction vertex determines the transverse vertex position. The visible energy in the calorimeter,  $E_{vis}$  is obtained by summing

the energy deposited in the scintillation counters from the interaction vertex to five counters beyond the end of the shower. The shower energy deposition profile is characterized by the ratio of the sum of the energy deposited in the first three scintillation counters to the total visible energy. Accordingly, we define

$$\eta_3 = 1 - \frac{E_1 + E_2 + E_3}{E_{vis}} \quad (2)$$

where  $E_i$  is the energy deposited in the  $i^{th}$  scintillation counter downstream of the interaction place.

The most downstream counter with energy deposited from the products of the neutrino interaction (CEXIT) occurs at the end of the hadron shower for  $\nu_\mu$  NC and  $\nu_e$  CC events but is determined by the muon track for most  $\nu_\mu$  CC events. We isolate the events without a muon track by requiring CEXIT to be no more than 10 counters downstream from the end of the hadron shower. We parametrize the event length which contains 99% of such events as:

$$L_{NC} = 4. + 3.81 \times \log(E_{vis}) \quad (3)$$

In order to measure the number of  $\nu_e$  CC events we divide the neutrino events into two classes: “short” if they deposit energy over an interval shorter than  $L_{NC}$ , and “long” otherwise. The long events consist almost exclusively of class 1 events, while the short ones are a mixture of class 2, class 3 and class 1 events with a low energy muon which cannot be separated on an event-by-event basis.

Based on Lund studies, we take the hadron showers produced in NC and CC interactions to be the same. Any difference in the shower energy deposition profile of long and short events is attributed to the presence of  $\nu_e$  CC interactions in the short sample. To compare directly the long and short events a muon track from the data was added to the short events to compensate for the absence of a muon in NC events. The fraction,  $f$ , of  $\nu_\mu$  CC events with a low energy muon contained in the short sample which now have two muon tracks was estimated from a detailed Monte Carlo of the experiment in the range of 20%. A simulated sample of such events was obtained by choosing long events with the appropriate energy distribution from the data to which a second short muon track was added in software. The length of the short track and the angular distribution were obtained from a Monte Carlo of  $\nu_\mu$  CC events.

To simulate  $\nu_e$  interactions in our detector we assume  $\nu_\mu - \nu_e$  universality. The electron neutrino showers were generated by adding a GEANT [9] generated electromagnetic shower of the appropriate energy to events in the long data sample. The energy distribution of the electron neutrinos and the fractional energy transfer  $y$  were generated using a detailed Monte Carlo simulation of the experiment. Since the hadron showers in the long sample

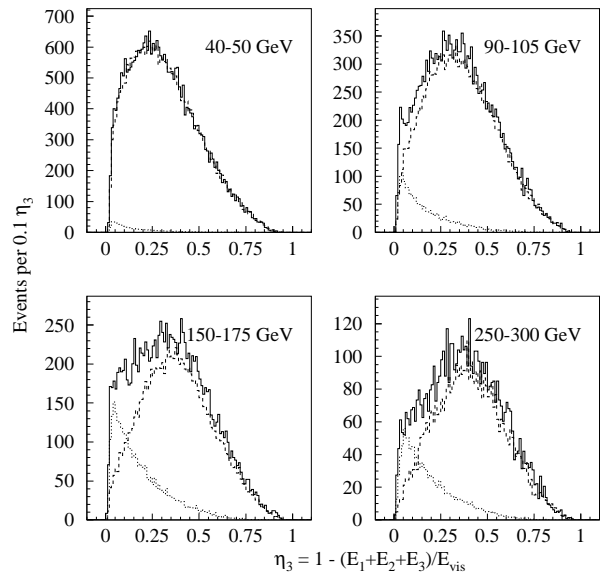


FIG. 2. Eta distributions for short (solid line), long (dashed line) and  $\nu_e$  (dotted line) events in four of the energy bins studied. The  $\nu_e$  and long distributions are normalized to the respective number of events predicted by the fit.

already have a muon track, the  $\nu_e$  sample can be compared directly with the short and long events.

The long and short  $\eta_3$  distributions were further corrected by subtracting the contamination due to cosmic ray events. The cosmic ray background was estimated from the event sample collected during a beam off gate using an identical analysis procedure as for the data gates. Additionally, the  $\eta_3$  distribution of short  $\nu_\mu$  CC events, normalized to the predicted fraction  $f$ , was subtracted from the short event sample. The  $\eta_3$  distributions for short, long, and  $\nu_e$  events for various energy bins are shown in Figure 2.

For this oscillation search we measure the absolute flux of  $\nu_e$ 's at the detector and compare it to the flux predicted by a detailed beamline simulation [10]. Any excess could be interpreted as a signal of  $\nu_\mu \rightarrow \nu_e$  oscillations. The  $\nu_\mu$  flux was determined directly from the low hadron energy CC event sample, normalized to the total neutrino cross-section [11]. The same beamline simulation is used to tag the creation point of each simulated  $\nu_\mu$  along the decay pipe, and give the number of predicted  $\nu_\mu$ 's at the detector normalized to the number observed at the detector divided by  $1 - P(\nu_\mu \rightarrow \nu_e)$ .  $P(\nu_\mu \rightarrow \nu_e) = P(\bar{\nu}_\mu \rightarrow \bar{\nu}_e)$  is the oscillation probability determined from eq. (1), assuming CP invariance. The predicted electron neutrino flux is normalized to the *produced* number of  $\nu_\mu$ 's. The  $\nu_e$  flux from neutrino oscillations is calculated by multiplying the *produced* number of  $\nu_\mu$ 's by  $P(\nu_\mu \rightarrow \nu_e)$ .

The events selected are required to deposit a minimum of 30 GeV in the target calorimeter to ensure complete efficiency of the energy deposition trigger. Additionally,

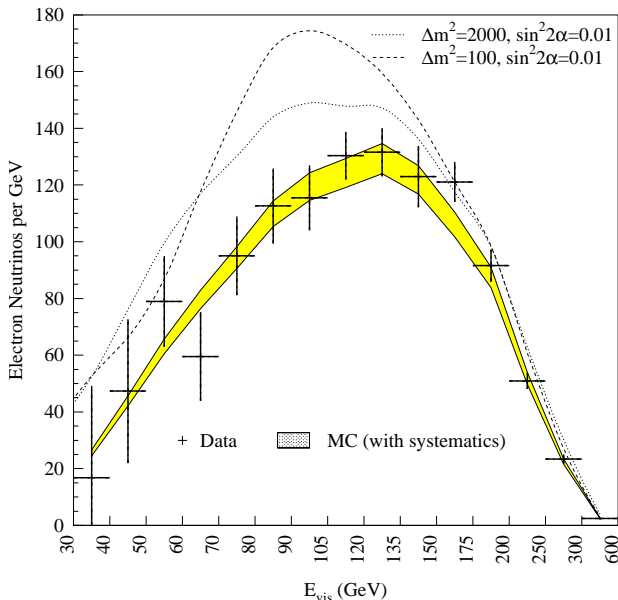


FIG. 3. Number of electron neutrinos as a function of visible energy. For electron neutrinos the visible energy is equal to the total neutrino energy. The filled band shows Monte Carlo prediction assuming no oscillations. The dotted curve corresponds to  $\nu_\mu \rightarrow \nu_e$  oscillations with  $\Delta m^2 = 2000 \text{ eV}^2$  and  $\sin^2 2\alpha = 0.01$  and the dashed curve to  $\Delta m^2 = 100 \text{ eV}^2$  and  $\sin^2 2\alpha = 0.01$

we require the event vertex to be more than 5 counters from the upstream end of the target and five counters plus the separation length from the downstream end and less than 50" from the detector centre-line. The resulting data sample consists of 632338 long events and 291354 short ones.

To extract the number of  $\nu_e$  CC events in each of 15  $E_{vis}$  bins, we fit the corrected shape of the observed  $\eta_3$  distribution for the short sample to a combination of  $\nu_\mu$  CC and  $\nu_e$  CC distributions with appropriate muon additions:

$$\nu_\mu \text{NC}(+\mu) = \alpha \nu_\mu \text{CC} + \beta \nu_e \text{CC}(+\mu) \quad (4)$$

The  $\chi^2$  of the fit in each of the 15  $E_{vis}$  bins ranges from 33.2 to 77.7 for 41 degrees of freedom (DoF) with a mean value of 48.4. Figure 3 shows that the measured number of  $\nu_e$  CC's agrees with the Monte Carlo prediction in each energy bin. The  $\chi^2$  value with a no-oscillations assumption is 9.97/15 DoF.

The major sources of uncertainties in the comparison of the electron flux extracted from the data to that predicted by the Monte Carlo are: (i) The statistical error from the fit in the extraction of the  $\nu_e$  flux. (ii) The error in the shower shape modeling, estimated by extracting the  $\nu_e$  flux using two definitions of  $\eta$ . Analogous to the definition of  $\eta_3$  given in eq. (2), we define  $\eta_4$  to be the ratio of the sum of the energy deposited outside the first four scintillation counters to the total visible energy. If

TABLE I. The result for  $\sin^2 2\alpha$  from the fit at each  $\Delta m^2$  for  $\nu_\mu \rightarrow \nu_e$  oscillations. The 90% C.L. upper limit is equal to the best fit  $\sin^2 2\alpha + 1.28\sigma$ .

$\Delta m^2 \text{ (eV}^2\text{)}$	Best fit	$\sigma$	$\Delta m^2 \text{ (eV}^2\text{)}$	Best fit	$\sigma$
1.0	-0.1741	1.6501	175.0	0.0000	0.0016
2.0	-0.0501	0.4107	200.0	-0.0002	0.0014
3.0	-0.0153	0.1852	225.0	-0.0003	0.0013
4.0	-0.0112	0.1041	250.0	-0.0004	0.0012
5.0	-0.0051	0.0671	275.0	-0.0004	0.0012
7.0	-0.0036	0.0345	300.0	-0.0004	0.0012
9.0	-0.0021	0.0213	350.0	-0.0004	0.0012
10.0	-0.0023	0.0173	400.0	-0.0003	0.0013
20.0	-0.0004	0.0048	450.0	-0.0003	0.0015
30.0	-0.0003	0.0026	500.0	-0.0004	0.0016
40.0	-0.0002	0.0018	600.0	-0.0005	0.0019
50.0	-0.0002	0.0015	700.0	-0.0003	0.0018
60.0	-0.0002	0.0014	800.0	-0.0002	0.0018
70.0	-0.0002	0.0014	1000.0	-0.0004	0.0017
80.0	-0.0003	0.0014	1500.0	-0.0003	0.0017
90.0	-0.0003	0.0015	2000.0	-0.0004	0.0017
100.0	-0.0002	0.0015	5000.0	-0.0003	0.0018
125.0	0.0004	0.0018	10000.0	-0.0004	0.0017
150.0	0.0005	0.0019	20000.0	-0.0004	0.0017

the modeling of the showers were correct, the difference in the number of electron neutrinos measured by the two methods should be small, any difference is used to estimate the systematic error. Since this error was shown not to be correlated among energy bins, we add it in quadrature to the statistical error from the fit and take this to be the combined basic error. (iii) The 1% uncertainty in the absolute energy calibration of the detector changes the relative neutrino flux which is extracted using the subset of the data sample with low hadron energy [11]. (iv) The uncertainty in the incident flux of  $\nu_e$ 's on the detector is estimated to be 4.1% [10]. This error is dominated by a 20% production uncertainty in the  $K_L$  content of the secondary beam which produces 16% of the  $\nu_e$  flux. The majority of the  $\nu_e$  flux comes from  $K_{e3}^\pm$  decays, which are well-constrained by the observed  $\nu_\mu$  spectrum from  $K_{\mu 2}^\pm$  decays [10]. Other sources of systematic errors were also investigated and found to be small.

The data are fit by forming a  $\chi^2$  which incorporates the Monte Carlo generated effect of oscillations, the basic error, and terms with coefficients accounting for systematic uncertainties. A best fit  $\sin^2 2\alpha$  is determined for each  $\Delta m^2$  by minimizing the  $\chi^2$  as a function of  $\sin^2 2\alpha$  and these systematic coefficients. At all  $\Delta m^2$ , the data are consistent with no observed  $\nu_\mu \rightarrow \nu_e$  oscillations. The statistical significance of the best-fit oscillation at any  $\Delta m^2$  is at most  $0.3\sigma$ .

The frequentist approach [12] is used to set a 90% confidence upper limit for each  $\Delta m^2$ . The limit in  $\sin^2 2\alpha$  corresponds to a shift of 1.64 units in  $\chi^2$  from the mini-

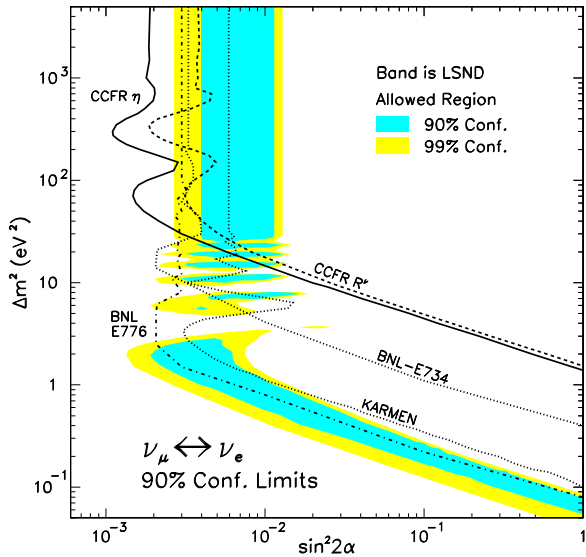


FIG. 4. Excluded region of  $\sin^2 2\alpha$  and  $\Delta m^2$  for  $\nu_\mu \rightarrow \nu_e$  oscillations from this analysis at 90% confidence is the area to the right of the dark, solid curve.

imum  $\chi^2$  (at the best fit value in Table I). The 90% confidence upper limit is plotted in Figure 4 for  $\nu_\mu \rightarrow \nu_e$ . The best limit of  $\sin^2 2\alpha < 1.1 \times 10^{-3}$  is at  $\Delta m^2 = 300 \text{ eV}^2$ . For  $\sin^2 2\alpha = 1$ ,  $\Delta m^2 > 1.6 \text{ eV}^2$  is excluded, and for  $\Delta m^2 \gg 1000 \text{ eV}^2$ ,  $\sin^2 2\alpha > 1.8 \times 10^{-3}$ .

Under the assumption that there are no oscillations, this data can also be used to test  $\nu_\mu(\bar{\nu}_\mu) \leftrightarrow \nu_e(\bar{\nu}_e)$  universality by comparing the observed  $\nu_e$  flux to that predicted by the Monte Carlo. From this comparison we determine the ratio of the cross sections averaged over our flux to be  $\sigma_{CC}(\nu_\mu)/\sigma_{CC}(\nu_e) = 1.026 \pm 0.055$ . This is currently the most stringent test of universality at high space-like momentum transfer.

In conclusion, we have used the difference in the longitudinal shower energy deposition pattern of  $\nu_e N$  versus  $\nu_\mu N$  interactions to search for  $\nu_\mu \rightarrow \nu_e$  oscillations with a coarse-grained calorimetric detector. We see a result consistent with no neutrino oscillations and find 90% confidence level excluded regions in the  $\sin^2 2\alpha - \Delta m^2$  phase space. This result is the most stringent limit to date for  $\nu_\mu \rightarrow \nu_e$  oscillation for  $\Delta m^2 > 25 \text{ eV}^2$ . We also tested  $\nu_\mu(\bar{\nu}_\mu) \leftrightarrow \nu_e(\bar{\nu}_e)$  universality and found the ratio of the  $\nu_\mu$ -to- $\nu_e$  cross-section to be  $1.026 \pm 0.055$ .

- [5] C. Athanassopoulos *et al.*, Phys. Rev. Lett. **77**, 3082 (1996).
- [6] K.S. McFarland, D. Naples *et al.*, Phys. Rev. Lett., **75**, 3993 (1995).
- [7] W.K. Sakumoto *et al.*, Nucl. Instrum. Methods, **A294**, 179 (1990).
- [8] B.J. King *et al.*, Nucl. Instrum. Methods, **A302**, 254 (1991).
- [9] CN/ASD, GEANT, detector description and simulation tool, CERN (1995).
- [10] C. Arroyo *et al.*, Phys. Rev. Lett. **72**, 3452 (1994); Bruce J. King, PhD Thesis, Columbia University (1994), Nevis preprint 284, unpublished.
- [11] P.Z. Quintas, PhD Thesis, Columbia University (1992), Nevis Preprint 277, unpublished; W.C. Leung, PhD Thesis, Columbia University (1991), Nevis Preprint 276, unpublished.
- [12] Particle Data Group, Phys. Rev. **D54**,164 (1996).

- 
- [1] B. Pontecorvo, JETP, **6**, 429 (1958); Z. Maki, M. Nakagawa and S. Sakata, Prog. Theor. Phys. **28**, 870 (1962).
  - [2] L. A. Ahrens *et al.*, Phys. Rev. **D36**, 702 (1987).
  - [3] L. Borodovsky *et al.*, Phys. Rev. Lett. **68**, 274 (1992).
  - [4] B.A. Bodmann *et al.*, Nucl. Phys. **A553**, 831c (1993).